# AHCYL2 (long-IRBIT) as a potential regulator of the electrogenic $Na^+$-$HCO_3^-$ cotransporter NBCe1-B

**Soichiro Yamaguchi[1, 2] and Toru Ishikawa[1, 3]**

[1]Laboratory of Physiology, Department of Biomedical Sciences, Graduate School of Veterinary Medicine, Hokkaido University, Sapporo, Japan

Present address: [2]Laboratory of Pharmacology, Department of Biomedical Sciences, Graduate School of Veterinary Medicine, Hokkaido University, Sapporo, Japan, [3]Department of Basic Veterinary Medicine, Division of Biomedical Science, Obihiro University of Agriculture and Veterinary Medicine, Obihiro 080-8555, Japan

Correspondence to Dr. Toru Ishikawa

Present Address: Department of Basic Veterinary Medicine, Division of Biomedical Science, Obihiro University of Agriculture and Veterinary Medicine, Obihiro 080-8555, Japan, Tel: 81-155-49-5356, Fax: 81-155-49-5356, Email: torui@obihiro.ac.jp

**ABSTRACT**

Although AHCYL2 (long-IRBIT) is highly homologous to IRBIT, which regulates ion-transporting proteins including the electrogenic $Na^+$-$HCO_3^-$ cotransporter NBCe1-B, its functions are poorly understood. Here, we found that AHCYL2 interacts with NBCe1-B in bovine parotid acinar cells using yeast two-hybrid, immunofluorescence confocal microscopy and co-immunoprecipitation analyses. Whole-cell patch-clamp experiments revealed that co-expression of AHCYL2 reduces the apparent affinity for intracellular $Mg^{2+}$ in inhibition of NBCe1-B currents specifically in a $HCO_3^-$-deficient cellular condition. Our data unveil AHCYL2 as a potential regulator of NBCe1-B in mammalian cells. We propose that cytosolic ionic condition appropriate for AHCYL2 to function might be different from IRBIT.

**KEY WORDS**

NBCe1-B, Long-IRBIT, IRBIT, intracellular $Mg^{2+}$, bovine parotid acinar cells, whole-cell patch-clamp

**ABBREVIATIONS**

AD, DNA-activation domain; AHCYL, Adenosylhomocysteine hydrolase-like protein; BD, DNA-binding domain; BPA, bovine parotid acinar; EGFP, enhanced green fluorescence protein; IB, immunoblot; IP, immunoprecipitation; $IP_3R$, Ins$P_3$ receptor; IRBIT, Ins$P_3$ receptor binding protein released with Ins$P_3$; NBCe, electrogenic $Na^+$-$HCO_3^-$ cotransporter; PLP, Paraformaldehyde/Lysine/Periodate; QDO, quadruple essential amino acids dropout; SD, synthetic dextrose; X-α-Gal, 5-bromo-4-chloro-3-indolyl-α-D-galactopyranoside.

## HIGHLIGHTS

- AHCYL2 is a novel binding partner of the N-terminus of NBCe1-B.
- AHCYL2 interacts with NBCe1-B in a native $HCO_3^-$-secreting exocrine gland.
- AHCYL2 lowers $Mg^{2+}$-sensitivity of NBCe1-B in a $HCO_3^-$-deficient cellular condition.
- Our data may uncover a novel role of AHCYL2 in the regulation of NBCe1-B.

## INTRODUCTION

NBCe1-B, a major splice variant of the electrogenic $Na^+$-$HCO_3^-$ cotransporter (NBCe1) operates with an apparent stoichiometry of 1 $Na^+$: 2 $HCO_3^-$ and plays essential roles in controlling intracellular pH in various cell types and epithelial $HCO_3^-$ secretion (1). NBCe1-B has a large cytosolic N-terminal region that is involved in protein-protein interactions with an inositol 1,4,5-trisphosphate (Ins$P_3$) receptor binding protein released with Ins$P_3$ (IRBIT) (2), a protein originally known as an interacting protein of Ins$P_3$ receptors ($IP_3R$) (3). IRBIT binds to the variant specific N-terminal region of NBCe1-B and regulates its cotransport rate (i.e. increase of per-molecule activity) (2, 4, 5). A serine-rich N-terminal region of IRBIT (PEST domain) that contains critical phosphorylation sites (6, 7) is essential for the interaction with NBCe1-B (2, 8). IRBIT enhances the cotransporter function mainly, but not exclusively, by relieving the N-terminal auto-inhibition that limits its intrinsic cotransport rate in *Xenopus* oocytes (5, 9).

When heterologously expressed in mammalian cells, NBCe1-B activity assessed by whole-cell patch-clamp is highly sensitive to intracellular $Mg^{2+}$ ($Mg^{2+}_i$) inhibition

that is likely immediate, reversible and mediated by electrostatic mechanism, and the $Mg^{2+}_i$ sensitivity is conferred partly by the variant specific N-terminal region (10). We have recently shown that IRBIT closely associates with NBCe1-B in bovine parotid acinar (BPA) cells (11), where endogenous NBCe1-B-like currents are much less sensitive to $Mg^{2+}_i$ inhibition than recombinant NBCe1-B currents under whole-cell voltage-clamp condition (10). Accordingly, heterologous co-expression of IRBIT reduces the apparent affinity for $Mg^{2+}_i$ in inhibition of NBCe1-B currents in HEK293 cells (11). However, we also noted that even when co-expressed with IRBIT, the NBCe1-B currents still had a higher sensitivity to $Mg^{2+}_i$ (11) compared to the native NBCe1-B-like currents (10). This has prompted us to search for additional cytosolic factors that might modify the $Mg^{2+}_i$ sensitivity of NBCe1-B in BPA cells.

In the present study, we performed a yeast two-hybrid screening of a bovine parotid cDNA library with the large cytosolic N-terminus of NBCe1-B as bait and identified AHCYL2 (adenosylhomocysteine hydrolase-like protein 2, also termed KIAA0828 or long-IRBIT) as a novel interacting partner. The N-terminus of AHCYL2 has homology with IRBIT including the highly conserved PEST domain except for N-terminal appendage (Long-IRBIT specific N-terminal domain) longer than that of IRBIT (12). However, AHCYL2 has been shown to retain little ability to interact with $IP_3R$ (13), and its functions have not been well elucidated compared to IRBIT (12).

Here, we show that AHCYL2 interacts with NBCe1-B in BPA cells using immunofluorescence confocal microscopy and co-immunoprecipitation analyses. We further demonstrate using the whole-cell patch-clamp technique that co-expression of AHCYL2 can regulate $Mg^{2+}_i$ sensitivity of recombinant NBCe1-B currents in a specific intracellular ionic setting.

## MATERIALS AND METHODS

*Animal material*

Bovine parotid tissue was obtained from a local slaughterhouse and Graduate School of Veterinary Medicine, Hokkaido University. Bovine parotid cells were enzymatically isolated as described previously (14).

*Yeast two-hybrid screening*

The MATCHMAKER library construction and screening kit (Takara Bio, Otsu, Japan) was used to construct a bovine parotid cDNA library. Bovine NBCe1-B was cloned from bovine parotid as described previously (14). The bait was constructed by cloning the cytosolic N-terminal region (amino acids 1 – 444) of the bovine NBCe1-B (NBCe1-B-Nt) into the pGBKT7 vector, encoding GAL4 DNA-activation domain (AD). The pGBK-NBCe1-B-Nt construct was transformed into the yeast strain Y187. The BD (cDNA library) and AD (NBCe1-B-Nt) constructs were introduced together through yeast mating, and positive transformants were further characterized and grouped by restriction mapping of PCR products generated for insert DNAs. Representative clones were sequenced and blasted against GenBank sequences. The interactions of NBCe1-B-Nt and IRBIT or AHCYL2 were re-tested using cDNA cloned from bovine parotid cells. AH109 yeast cells were co-transformed with pGBKT7 vectors, which contained either NBCe1-B-Nt, or no insert and pGADT7 vectors, which contained IRBIT, AHCYL2, or no insert.

*Cloning of AHCYL2 from bovine parotid*

mRNA was extracted from enzymatically isolated bovine parotid cells and first-strand cDNA was generated from mRNA using SuperScript II RT (Life Technologies). The specific oligonucleotide primers for PCR for bovine AHCYL2 were derived from the sequences obtained from yeast two-hybrid screening. The AHCYL2 sense primer was 5'- GCG GTG ATG TCG GTG CAG GTC GTG T -3' and the antisense primer was 5'- CCA GAA AAC CCC AGA AAA CAA GGA G -3'. The size of the expected fragments of AHCYL2 was 2210 bp, which encoded their all of open reading frames. The PCR reaction was performed with TaKaRa LA Taq (Takara Bio). The PCR conditions were: denaturation 94 °C for 30 sec; annealing 64 °C for 30 sec; extension 72 °C for 3 min; 35 cycles.

PCR products of AHCYL2 amplified using a high fidelity enzyme, PrimeSTAR HS DNA Polymerase (Takara Bio) or Pfu-Turbo (Stratagene, LaJolla, CA, USA) were subcloned into pGADT7, pIRES2-EGFP, or pEGFP-C1vector and used for following experiments.

*Cell Transfection*

The plasmid encoding AHCYL2, IRBIT, or empty vector pIRES2-EGFP was transiently transfected using Lipofectamine 2000 (Life Technologies) into HEK293 cells stably expressing NBCe1-B (pCIneo mammalian expression vector, Promega, Madison, WI, USA) (14). Patch-clamp recordings were made two days after transfection from EGFP positive single cells, which exhibited strong fluorescence.

*Western Blot*

Isolated bovine parotid cells and HEK293 cells stably expressing NBCe1-B that were

transfected with each construct (i.e. bovine AHCYL2 or IRBIT subcloned into pIRES2-EGFP vector or vector alone) were lysed in a buffer containing a protease inhibitor cocktail (1/100 dilution, Sigma P8340). Bovine parotid protein (5 μg) and transfected HEK293 cell protein (20 μg) were separated by SDS-PAGE and transferred to nitrocellulose paper. After incubation in blocking buffer, the blots were treated with the diluted rabbit anti-NBCe1 antibody (1:10,000, Chemicon International, Temecula, CA, USA), rabbit anti-AHCYL2 antibody (1:10,000, Bethyl laboratories, Inc., Montgomery, TX, USA), or mouse anti-IRBIT antibody (1:5,000, Abnova, Taipei, Taiwan) and then with horseradish peroxidase-conjugated anti-rabbit or anti-mouse IgG antibody (1:10,000, GE Healthcare, Buckinghamshire, UK) as the secondary antibody. The signal was detected by an ECL Plus system and ECL mini-camera (GE Healthcare).

*Co-immunoprecipitation*

Isolated bovine parotid cells were suspended in lysis buffer for co-immunoprecipitation. Briefly, the homogenized suspension was precleared and immunoprecipitated with the following antibodies; rabbit anti-AHCYL2 antibody (5 μg, Bethyl), mouse anti-IRBIT antibody (5 μl of serum, Abnova), rabbit anti-NBCe1 antibody (5 μl of serum, Chemicon), control normal mouse IgG (5 μg, Sigma), or control normal rabbit IgG (5 μg, sigma). The mixtures were added to the homogeneous protein A-suspension (50 μl) and incubated for overnight at 4 °C. After washes, immunoprecipitated proteins were analyzed by SDS-polyacrylamide gel electrophoresis and western blot.

*Immunofluorescence confocal microscopy*

Isolated bovine parotid cells were fixed in PLP fixative overnight at 4 °C, and

permeabilized with 1% SDS in phosphate-buffered saline (PBS) for 5 min. After blocked in image-iT signal enhancer (Life Technologies) and in PBS containing 5% normal goat serum and 0.2% BSA, the cells were incubated with rabbit anti-AHCYL2 antibody (1 μg/ml, Bethyl), mouse anti-IRBIT antibody (1:500, Abnova), and/or mouse anti-NBCe1 antibody (1:1,000, Abnova, H00008671-A01), and then with Alexa 488-conjugated goat anti-mouse IgG and/or Alexa 594-conjugated goat anti-rabbit IgG (1:500, Life Technologies). The coverslips were observed under IX-70 confocal fluorescence microscopy (Olympus, Tokyo, Japan) with a 60× oil-immersion objective.

*Electrophysiology*

Whole-cell patch-clamp experiments were performed at room temperature and NBCe1-B currents were defined as the extracellular $Na^+$-dependent currents at 0 mV as described previously (10, 11).

All average results are presented as mean ± SE of independent experiments (n), where n refers to the number of cells tested.

For detailed information, see Supplemental materials on line.

**RESULTS**

*Identification of AHCYL2 as a novel binding partner of NBCe1-B using the yeast two-hybrid system*

We performed a yeast two-hybrid screening of a bovine parotid cDNA library using the first 444 amino acid residues of the cytosolic N-terminal region of bovine NBCe1-B as bait and identified AHCYL2 as a potential binding partner of NBCe1-B. One colony among 170 colonies tested included the vector encoding full length

AHCYL2. Full length IRBIT was also detected by the screening (11 colonies) as mentioned briefly in a previous report (see *Materials and Methods* of (11)). The interaction between the NBCe1-B N-terminal region and AHCYL2 or IRBIT in yeast was confirmed by co-transformation of AH109 yeast cells with pGBKT7 vector encoding N-terminal region of NBCe1-B and pGADT7 vector encoding AHCYL2 or IRBIT (Fig.1).

*Bovine parotid cells express AHCYL2*

RT-PCR analysis showed that bovine parotid cells express the transcripts of AHCYL2 (Fig. 2A). The nucleotide sequence of open reading frame of obtained bovine parotid AHCYL2 was almost identical to a reported sequence of bovine AHCYL2 (Genebank accession #: NM_001101143.1), except that it differed from the reported amino acid sequence (NP_001094613.1) by missing three nucleotides encoding Q122. It is noteworthy that human (NP_001124192.1) and mouse (NP_001164471.1) AHCYL2 do not contain the glutamine either. The homology of amino acid sequence between bovine and human or mouse AHCYL2 is 99% or 97%, respectively.

Western blot analysis showed that bovine parotid cells express the proteins of AHCYL2 (Fig. 2B). The anti-IRBIT antibody and anti-AHCYL2 antibody used were confirmed to specifically recognize IRBIT and AHCYL2 exogenously expressed in HEK293 cells, respectively (Fig. 2B). The additional slower-migrating band of AHCYL2 may be due to the phosphorylation of LISN (Long-IRBIT specific N-terminal) domain in AHCYL2 (13).

*AHCYL2 closely associates with NBCe1-B and IRBIT in bovine parotid acinar (BPA)*

*cells*

The expression of AHCYL2, NBCe1-B, or IRBIT in isolated bovine parotid cells was evaluated by immunofluorescence confocal microscopy. Double immunolabeling for AHCYL2 and NBCe1-B (Fig. 3A) or IRBIT (Fig. 3B) showed that AHCYL2, NBCe1-B, and IRBIT are co-expressed in acinar cells. Immunofluorescence staining pattern of NBCe1-B overlapped with that of AHCYL2 (Fig. 3A). AHCYL2 and IRBI also had overlapping distributions (Fig. 3B). The specificities of these staining of AHCYL2 and NBCe1-B were confirmed by antigen pre-absorption experiments (Fig. 3C) as shown for those of IRBIT and NBCe1-B in a previous report (11).

In heterologous co-expression experiments, we found that as NBCe1-B, AHCYL2 was present in proximity to regions of the plasma membranes of HEK293 cells, but such localization pattern of AHCYL2 was not observed when AHCYL2 was expressed alone (Supplemental Fig. S1). Therefore, the AHCYL2 expression in proximity to the plasma membranes of BPA cells may depend on the membrane expression of NBCe1-B.

AHCYL2 was co-immunoprecipitated with NBCe1-B from bovine parotid cell lysate and vice versa (Fig. 4, IP: anti NBCe1 and IP: anti AHCYL2). Three out of four experiments showed the same results. An anti-AHCYL2 antibody also immunoprecipitated IRBIT (Fig. 4, IP anti AHCYL2, IB: IRBIT), suggesting that AHCYL2 may form heteromultimer with IRBIT in BPA cells. This suggestion appeared to be consistent with the observation that IRBIT and AHCYL2 co-localized in BPA cells (Fig. 3B). However, AHCYL2 was not precipitated with an anti-IRBIT antibody (Fig. 4, IP: anti IRBIT, IB: AHCYL2) and neither was NBCe1-B as reported elsewhere (11). The reason for these observations is unclear at this stage. It might be simply because the antibody did not precipitate a sufficient amount of IRBIT proteins to detect binding

partners as the band of precipitated IRBIT was relatively faint (Fig. 4, IP: anti IRBIT, IB: IRBIT). Alternatively, concerning the binding with AHCYL2, a large fraction of IRBIT might be homomultimer by itself, because in many tissues expression level of IRBIT has been shown to be higher than that of AHCYL2 (13). Control IgG did not precipitate NBCe1-B, AHCYL2, and IRBIT, neither.

*AHCYL2 can regulate intracellular $Mg^{2+}$-sensitivity of NBCe1-B in a $HCO_3^-$-deficient cellular condition*

To examine whether AHCYL2 would modify the $Mg^{2+}{}_i$-sensitivity of NBCe1-B as IRBIT did (11), we transiently transfected AHCYL2 or empty vector alone into HEK293 cells stably expressing NBCe1-B and measured NBCe1-B currents. NBCe1-B current densities were evaluated as the extracellular $Na^+$-dependent currents at 0 mV under the presence of extracellular $HCO_3^-$ in order especially to minimize the influence of back ground leakage currents as described previously (10, 11). We first dialyzed the cells using a pipette solution with added 25 mM $HCO_3^-$, an experimental condition, under which IRBIT was effective in changing the sensitivity of NBCe1-B to $Mg^{2+}{}_i$ inhibition (11). We found no difference in dose-inhibition curves for $Mg^{2+}{}_i$ in between AHCYL2- and mock-transfected cells (Supplemental Figure S2). However, intriguingly, when dialyzed with a nominally $HCO_3^-$-free pipette solution, these transfected cells exhibited NBCe1 currents with different $Mg^{2+}{}_i$-sensitivities. When a nominally $HCO_3^-$- and $Mg^{2+}$-free pipette solution was used to dialyze the cells, the NBCe1-B currents were not affected by co-expression of AHCYL2 (control: 3.5 ±0.8 pA/pF (n = 4) and +AHCYL2: 3.2 ±1.0 pA/pF (n = 6) at 0 mV, Fig. 5A). On the other hand, when the cells were dialyzed with a pipette solution having $10^{-4}$ M of free $Mg^{2+}$, the NBCe1-B

currents were increased by co-expression of AHCYL2 (control: 0.3 ±0.3 pA/pF (n = 5) and +AHCYL2: 4.6 ±1.3 pA/pF (n = 7) at 0 mV, Fig. 5A). Co-expression of AHCYL2 caused a rightward shift of the dose-response curve for $Mg^{2+}_i$ inhibition, such that $Mg^{2+}_i$-sensitivity for NBCe1-B current recorded from AHCYL2-transfected cells was estimated to be approximately 100-fold lower than that from mock-transfected cells (Fig. 5B). The data suggest that AHCYL2 may reduce the $Mg^{2+}_i$ sensitivity of NBCe1-B depending upon cytosolic $HCO_3^-$ levels.

Given a functional interaction between AHCYL2 and NBCe1-B suggested in a model cell system, we hypothesized that $Mg^{2+}_i$-sensitivity of native NBCe1-B-like currents in BPA cells may be also lower in the nominal absence of $HCO_3^-{}_i$, compared to the presence of $HCO_3^-{}_i$. We subsequently examined the $Mg^{2+}_i$-sensitivity of native NBCe1-B-like currents in BPA cells using a pipette solution with no added $HCO_3^-$ and compared its dose-response curve for $Mg^{2+}_i$ inhibition with that previously determined using a solution with added 25 mM $HCO_3^-$ (10). NBCe1-B-like currents recorded with the nominally $HCO_3^-$-free pipette solution were inhibited by intracellular $Mg^{2+}$ in a concentration-dependent manner, and an apparent $K_i$ value was estimated to be 4.3 $\times 10^{-3}$ M (Supplemental Figure S3). This value was approximately 5-fold higher than that (8.17 $\times 10^{-4}$ M) estimated using pipette solutions with added 25 mM $HCO_3^-$ (10).

## DISCUSSION

In the present study, we identified AHCYL2 (long-IRBIT) as a novel binding partner of the cytosolic N-terminus of NBCe1-B and subsequently showed that AHCYL2 forms a molecular complex with NBCe1-B in BPA cells. We also showed that heterologous co-expression of AHCYL2 did reduce the $Mg^{2+}_i$-sensitivity of NBCe1-B

currents in HEK293 cells when the cells were dialyzed with pipette solutions with no added $HCO_3^-$, but not solutions with added 25 mM $HCO_3^-$. These results together with our recent work on IRBIT (11) suggest that AHCYL2 can modify $Mg^{2+}_i$ sensitivity of NBCe1-B as IRBIT does, but intracellular ionic condition appropriate for AHCYL2 to function may be different from IRBIT.

Our immunofluorescence confocal microscopy and co-immunoprecipitation data suggest that AHCYL2 and IRBIT may form hetero-multimer in BPA cells (Fig. 4). The conclusion is consistent with that drawn by a previous study (13). Besides, although we did not compare the expression level between AHCYL2 and IRBIT in BPA cells, the quantity of colonies detected by yeast two-hybrid screening (1 AHCYL2 colony and 11 IRBIT colonies) implies that the expression level of AHCYL2 is lower than that of IRBIT as reported for other tissues (13). Therefore, we cannot completely exclude the possibility that IRBIT intermediates the binding between NBCe1-B and AHCYL2 in BPA cells. Nevertheless, unless yeasts express endogenous IRBIT substantially, the results of yeast two-hybrid screening would suggest that AHCYL2 can bind to NBCe1-B directly.

In the present study, we found that NBCe1-B was co-immunoprecipitated with AHCYL2, but not with IRBIT from bovine parotid cell lysate (Fig. 4, (11)), although both AHCYL2 and IRBIT were co-immunoprecipitated with NBCe1-B. Because unlike IRBIT, AHCYL2 cannot bind to $IP_3R$ (13), more free form of AHCYL2, compared to that of IRBIT, might be available for binding to NBCe1-B especially under non-stimulated resting condition, where Ins$P_3$ concentration is expected to be low in the cells. It remains unclear at this stage if AHCYL2 competes with IRBIT toward a binding site of NBCe1-B and if the relief of $Mg^{2+}_i$ inhibition by IRBIT is also affected

by intracellular $HCO_3^-$. It is tempting to speculate that intracellular $HCO_3^-$ concentration could act as a "switch" initiating or terminating regulatory machinery operated by AHCYL2 and thus determine the relative contributions of AHCYL2 and IRBIT to the regulation of NBCe1-B.

At present, the mechanism by which AHCYL2 changes the $Mg^{2+}_i$-sensitivity of NBCe1-B only when intracellular $HCO_3^-$ concentration ($[HCO_3^-]_i$) is minimal remains unknown. We speculate that $HCO_3^-{}_i$ might be a cytosolic factor that causes conformational change of AHCYL2 and/or NBCe1-B and thus regulates their interaction. Further studies will be needed to address this issue specifically by examining whether intracellular $HCO_3^-$ concentration could affect binding affinity of AHCYL2 to NBCe1-B, because the present co-immunoprecipitation experiments were done under a nominally $HCO_3^-$-free condition.

AHCYL2 regulation of NBCe1-B activity under a limited cellular condition (i.e. low $[HCO_3^-]_i$) may have physiological and/or pathophysiological impacts on intracellular $HCO_3^-$ (and thus pH) homeostasis and epithelial $HCO_3^-$ secretion whether or not it takes place in collaboration with and/or in preference to IRBIT. For example, when $[HCO_3^-]_i$ becomes low, AHCYL2 might activate NBCe1-B by reducing its $Mg^{2+}_i$-sensitivity and thus increase $[HCO_3^-]_i$ that in turn makes AHCYL2 less effective in controlling the cotransporter activity. This type of regulation would also ensure the optimal $[HCO_3^-]_i$ for $HCO_3^-$ secretion. From this view point, it is noteworthy that $Mg^{2+}_i$-sensitivity of native NBCe1-B-like currents in BPA cells dialyzed with the nominally $HCO_3^-$-free pipette solution was indeed lower than that of the currents from BPA cells dialyzed with the $HCO_3^-$-containing one (Supplemental Figure S3). Once primary cultures of BPA cells that preserve the properties of NBCe1-B are successfully

established, it would be interesting to test whether knock-down of endogenous AHCYL2 affects $HCO_3^-{}_i$-dependent modification of $Mg^{2+}{}_i$-sensitivity of native NBCe1-B-like currents in these cells.

**REFERENCES**


1. Romero MF, Chen AP, Parker MD & Boron WF (2013). The SLC4 family of bicarbonate ($HCO_3^-$) transporters. *Mol Aspects Med* **34,** 159-182.

2. Shirakabe K, Priori G, Yamada H, Ando H, Horita S, Fujita T, Fujimoto I, Mizutani A, Seki G & Mikoshiba K (2006). IRBIT, an inositol 1,4,5-trisphosphate receptor-binding protein, specifically binds to and activates pancreas-type $Na^+/HCO_3^-$ cotransporter 1 (pNBC1). *Proc Natl Acad Sci U S A* **103,** 9542-9547.

3. Ando H, Mizutani A, Matsu-ura T & Mikoshiba K (2003). IRBIT, a novel inositol 1,4,5-trisphosphate ($IP_3$) receptor-binding protein, is released from the $IP_3$ receptor upon $IP_3$ binding to the receptor. *J Biol Chem* **278,** 10602-10612.

4. Yang D, Li Q, So I, Huang CL, Ando H, Mizutani A, Seki G, Mikoshiba K, Thomas PJ & Muallem S (2011). IRBIT governs epithelial secretion in mice by antagonizing the WNK/SPAK kinase pathway. *J Clin Invest* **121,** 956-965.

5. Lee SK, Boron WF & Parker MD (2012). Relief of autoinhibition of the

electrogenic Na-HCO(3)[corrected] cotransporter NBCe1-B: role of IRBIT vs. amino-terminal truncation. *Am J Physiol Cell Physiol* **302,** C518-526.

6. Ando H, Mizutani A, Kiefer H, Tsuzurugi D, Michikawa T & Mikoshiba K (2006). IRBIT suppresses $IP_3$ receptor activity by competing with $IP_3$ for the common binding site on the $IP_3$ receptor. *Mol Cell* **22**, 795-806.

7. Devogelaere B, Beullens M, Sammels E, Derua R, Waelkens E, van Lint J, Parys JB, Missiaen L, Bollen M & De Smedt H (2007). Protein phosphatase-1 is a novel regulator of the interaction between IRBIT and the inositol 1,4,5-trisphosphate receptor. *Biochem J* **407,** 303-311.

8. Yang D, Shcheynikov N, Zeng W, Ohana E, So I, Ando H, Mizutani A, Mikoshiba K & Muallem S (2009). IRBIT coordinates epithelial fluid and $HCO_3^-$ secretion by stimulating the transporters pNBC1 and CFTR in the murine pancreatic duct. *J Clin Invest* **119,** 193-202.

9. McAlear SD, Liu X, Williams JB, McNicholas-Bevensee CM & Bevensee MO. (2006). Electrogenic Na/$HCO_3$ Cotransporter (NBCe1) Variants Expressed in Xenopus Oocytes: Functional Comparison and Roles of the Amino and Carboxy Termini. *J Gen Physiol* **127,** 639-658.

10. Yamaguchi S & Ishikawa T (2008). The electrogenic $Na^+$-$HCO_3^-$ cotransporter NBCe1-B is regulated by intracellular $Mg^{2+}$. *Biochem Biophys Res Commun*

**376,** 100-104.

11. Yamaguchi S & Ishikawa T (2012). IRBIT reduces the apparent affinity for intracellular $Mg^{2+}$ in inhibition of the electrogenic $Na^{+}$-$HCO_3^{-}$ cotransporter NBCe1-B. *Biochem Biophys Res Commun* **424**, 433-438.

12. Devogelaere B, Sammels E & De Smedt H. (2008). The IRBIT domain adds new functions to the AHCY family. *Bioessays* **30,** 642-652.

13. Ando H, Mizutani A & Mikoshiba K (2009). An IRBIT homologue lacks binding activity to inositol 1,4,5-trisphosphate receptor due to the unique N-terminal appendage. *J Neurochem* **109,** 539-550.

14. Yamaguchi S & Ishikawa T (2005). Electrophysiological characterization of native $Na^{+}$-$HCO_3^{-}$ cotransporter current in bovine parotid acinar cells. *J Physiol* **568,** 181-197.

## ACKNOWLEDGEMENT

S. Yamaguchi was supported by a JSPS Research Fellowship for Young Scientists.

## FIGURE LEGENDS

**Figure 1. Interaction of NBCe1-B and AHCYL2 or IRBIT in yeast two-hybrid system**

Interaction of full-length AHCYL2 or IRBIT and N-terminal region (amino acids 1-444) of NBCe1-B (NBCe1-B-Nt) as shown by yeast two-hybrid analysis. Yeast cells were co-transformed with pGADT7-AHCYL2, pGADT7-IRBIT or empty pGADT7 along with pGBKT7-NBCe1-B-Nt or empty pGBKT7 as indicated. Two control strains were produced by co-transformation with pGADT7-RecT along with pGBKT7-53 (Positive control) or pGBKT7-Lam (Negative control). About $2.3 \times 10^5$ cells, each of these transformed yeasts, were dropped and grown on a SD–Leu/–Trp/X-α-Gal plate and a SD QDO (–Ade/–His/–Leu/–Trp)/X-α-Gal plate. Blue color indicates the activation of *lacZ* gene induced by interaction of two proteins encoded in vectors.

**Figure 2. Expression of AHCYL2 in bovine parotid**

*A*, detection of mRNA transcripts of AHCYL2 from bovine parotid cDNA by RT-PCR. Lane M: size markers (Stable 1 kbp DNA ladder, Sigma). RT, reverse transcription. The size of the expected fragments of AHCYL2 was 2210 bp. *B*, immunoblotting detection of IRBIT and AHCYL2 in bovine parotid cells and bovine NBCe1-B-expressing HEK293 cells transiently transfected with IRBIT, AHCYL2, or empty vector (pIRES2-EGFP). The antibody against IRBIT or AHCYL2 specifically recognized IRBIT or AHCYL2, respectively. The data with anti-IRBIT antibody except for NBCe1-B-expressing HEK293 cells transiently transfected with AHCYL2 were the same as reported previously (11).

**Figure 3. Co-expression of AHCYL2, IRBIT, and NBCe1-B in dissociated BPA cells**

Dissociated bovine parotid cells were double-stained with antibodies against AHCYL2 and NBCe1 (A) or IRBIT (B). As negative controls, cells were stained with antigen-preabsorbed antibodies (C). Alexa 488 goat anti-mouse IgG antibody and Alexa 594 goat anti-rabbit IgG antibody were used for secondary antibodies. Nuclei of the cells were stained with Hoechst 33342 (Blue). Yellow shows the overlap of the signals indicated green and red (merge). Specificity of anti-IRBIT antibody was confirmed previously (11). Scale bars: 10 μm.

**Figure 4. Co-immunoprecipitation of AHCYL2, IRBIT, and NBCe1-B**

Bovine parotid lysates were immunoprecipitated with an anti-AHCYL2, anti-IRBIT, anti-NBCe1, or control antibody. The immunoprecipitates were subjected to western blotting and probed with anti-NBCe1 (top), anti-AHCYL2 (middle), or anti-IRBIT (bottom) antibody. Total lysate was also loaded (input). The smear around the band of immunoprecipitated NBCe1-B (IP: anti NBCe1, IB: NBCe1) might be due to aggregation and degradation of the protein. IP: immunoprecipitation, IB: immunoblot.

**Figure 5. AHCYL2 reduces $Mg^{2+}_i$ sensitivity of NBCe1-B**

*A*. Whole-cell current density evoked by ramp pulse protocol is shown at 10-mV intervals from -90 mV to 40 mV in 25 mM $HCO_3^-$ containing $Na^+$-rich (open circles) or $Na^+$-free (solid circles) bath solutions. Empty vector (a, pIRES2-EGFP) or a vector encoding AHCYL2 (b) was transiently transfected into HEK293 cells stably expressing

NBCe1-B (pCIneo). $Mg^{2+}$-free (lower) or $10^{-4}$ M $Mg^{2+}$-containing (upper) pipette solution was used. Shown are mean ± S.E. (n = 4-7). *B*. Dose-response relation for $Mg^{2+}_i$ inhibition of NBCe1-B currents recorded from the cells expressing NBCe1-B alone (open circles) or with AHCYL2 (solid circles). The line for the control data (open circles) is a fit to the Hill equation ($K_i$ value: 1.0 $\times 10^{-5}$ M; Hill coefficient: 0.95), whereas the line for the data obtained from the cells transfected with AHCYL2 (solid circles) is derived from the Hill equation with self-defined values ($K_i$ value: 8.9 $\times 10^{-4}$ M; Hill coefficient: 1.45), because the data were unable to be fitted with a computer program properly. Shown are mean ± S.E. (n = 6 or 7 AHCYL2, n = 4 or 5 control)

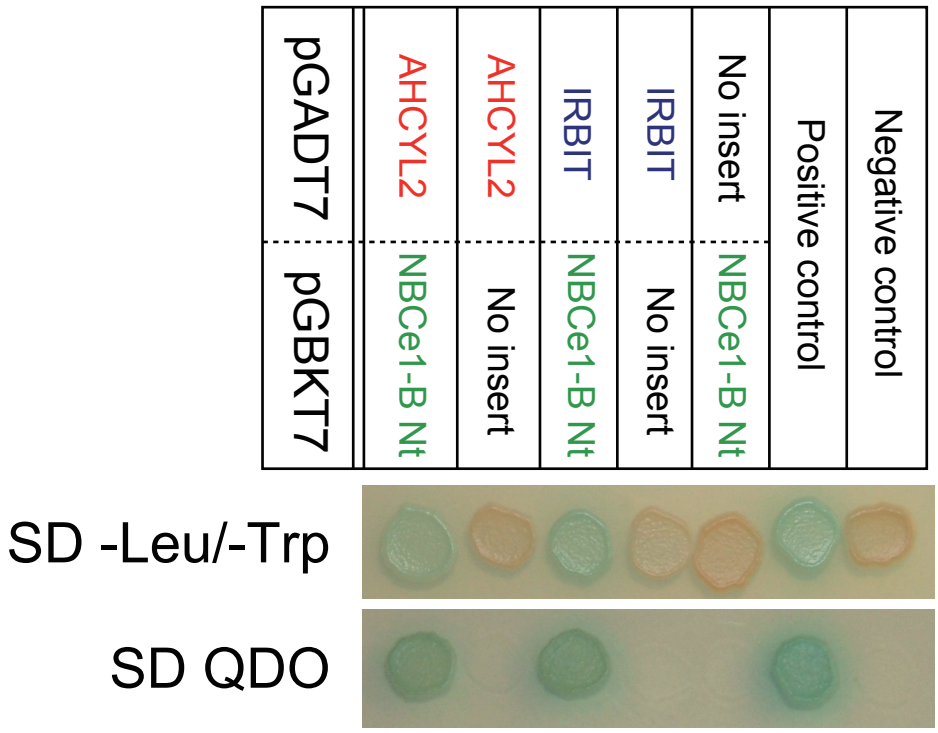


Figure 1 Yamaguchi S. and Ishikawa T.

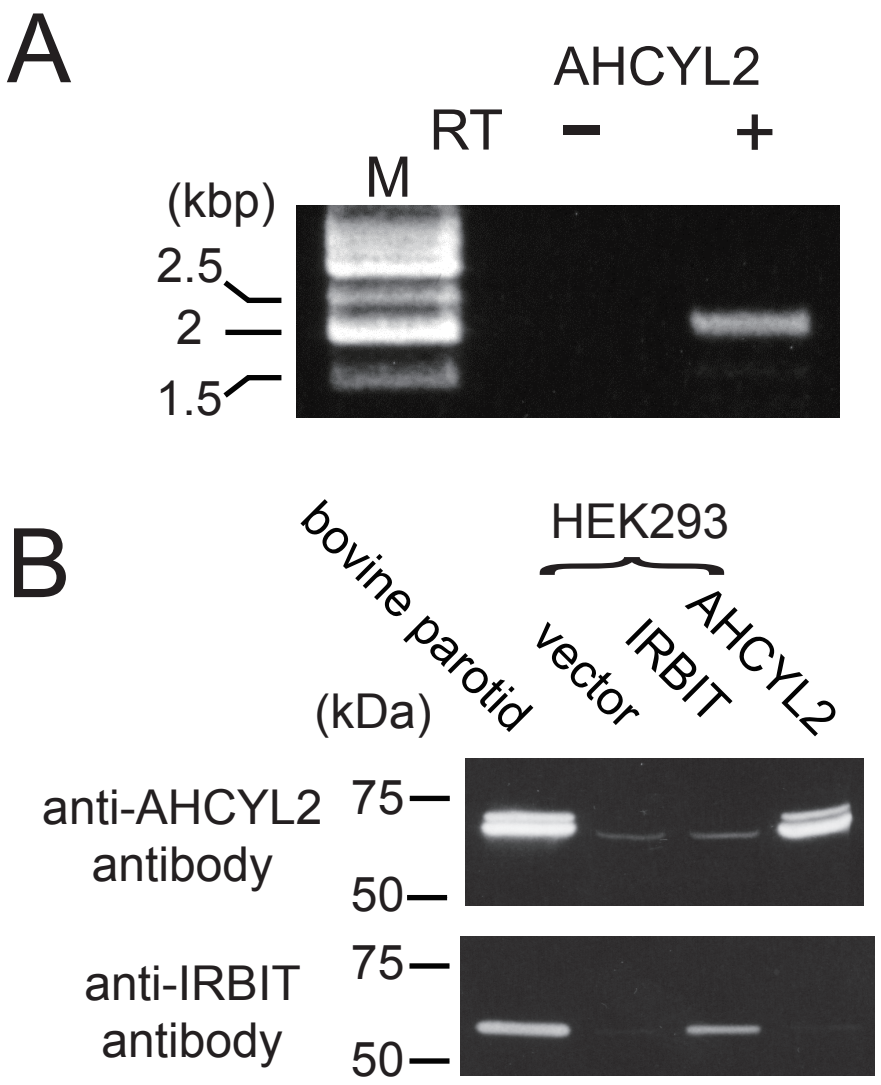


Figure 2 Yamaguchi S. and Ishikawa T.

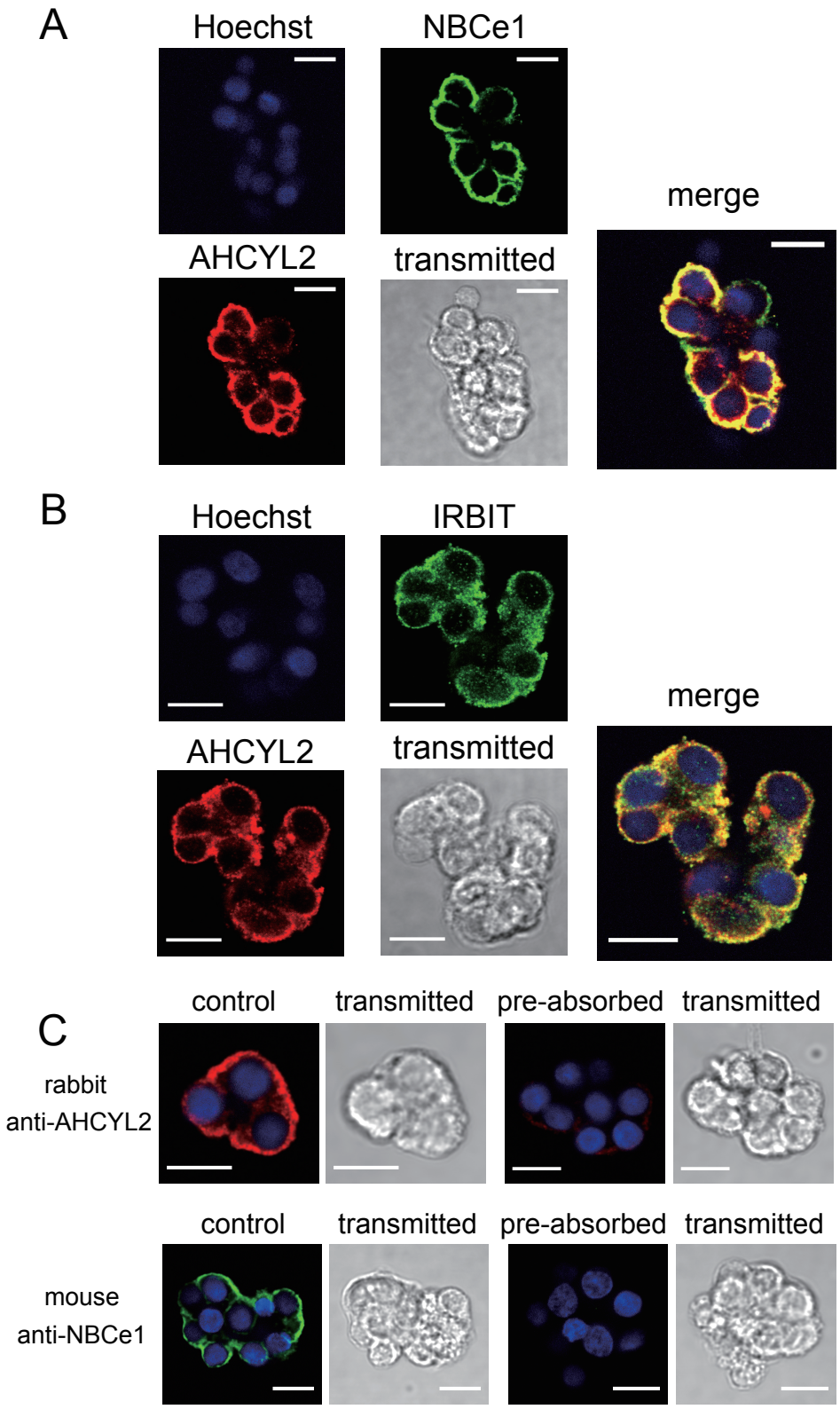


Figure 3 Yamaguchi S. and Ishikawa T.

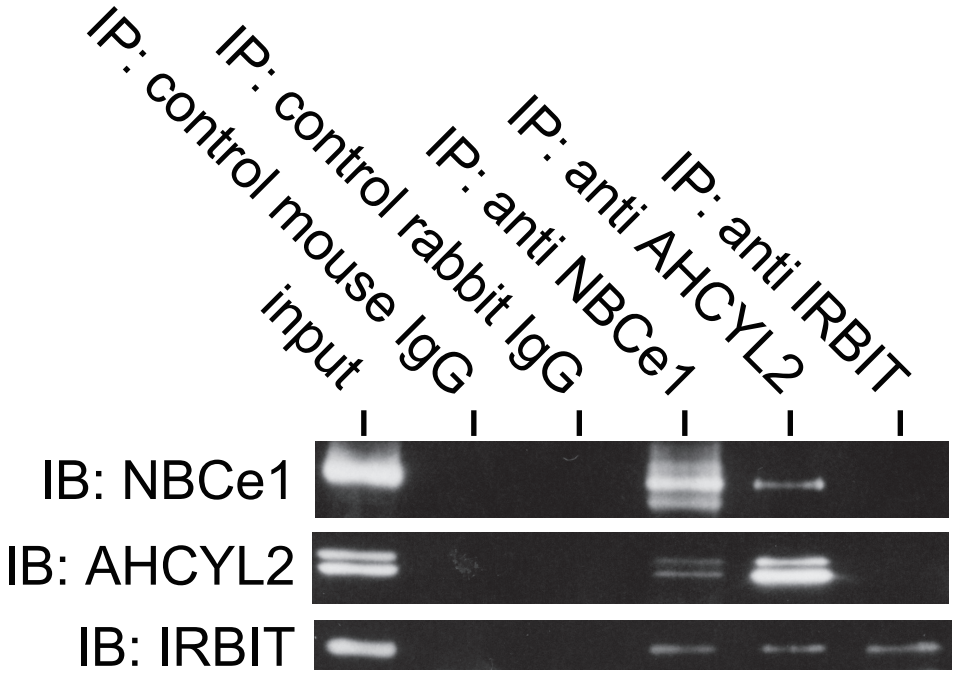


Figure 4 Yamaguchi S. and Ishikawa T.

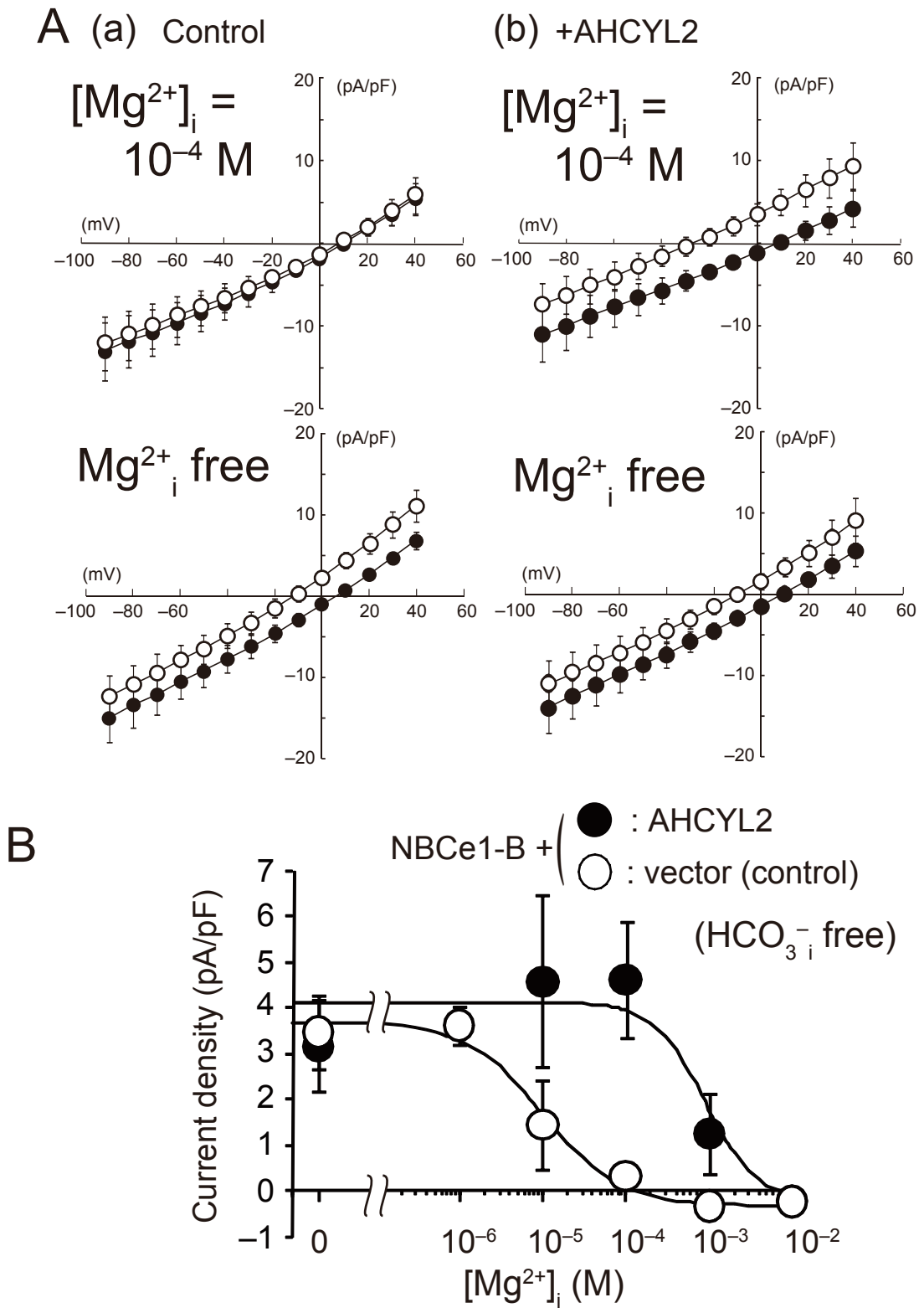


Figure 5 Yamaguchi S. and Ishikawa T.